

IMPROVED ENERGY CONFINEMENT AT TRANS- GREENWALD DENSITIES IN DISCHARGES WITH A RADIATING EDGE IN THE TOKAMAK TEXTOR-94

B.Unterberg 1), G.Mank 1), A.M.Messiaen 2), J.Ongena 2), S.Brezinsek 1), V.Dreval 4), P.Dumortier 2), R.Jaspers 3), D.Kalupin 2), H.R.Koslowski 1), A.Krämer-Flecken 1), A.Kreter 1), M.Lehnen 1), A.Pospieszczyk 1), J.Rapp 1), U.Samm 1), B.Schweer 1), G.Sergienko 1), S.Soldatov 4), M.Z.Tokar' 1), G.Van.Wassenhove 2), R.R.Weynants 2) and the TEXTOR-94 Team 1),2),3)

1) Institut für Plasmaphysik, Forschungszentrum Jülich, Ass. "EURATOM- FZ Jülich", D-52425 Jülich, Germany *

2) Laboratoire de Physique des Plasmas – Laboratorium voor Plasmafysica, Ass. "EURATOM- Belgian State", ERM- KMS, B- 1000 Brussels, Belgium *

3) FOM Instituut voor Plasmafysica Rijnhuizen, Ass. " EURATOM-FOM", NL-3430 BE, Nieuwegein, The Netherlands *

4) Nuclear Fusion Institute, Russian Research Centre "Kurchatov Institute", Kurchatov Square 1, 123182 Moscow, Russia

* Partners in the Trilateral Euregio Cluster

Email of corresponding author: B.Unterberg@fz-juelich.de

Abstract. Confinement quality as good as in the ELM-free H-mode at plasma densities substantially above the Greenwald density (up to $\bar{n}_e/n_{GW} = 1.4$) has been obtained in discharges with a radiating boundary in the tokamak TEXTOR-94. This is achieved by optimising the gas fuelling rate of RI-mode discharges to avoid both a confinement back transition at the beta limit or a confinement degradation to L-mode levels as a consequence of a too strong gas puffing. A successful increase of the density to values well above n_{GW} without degradation is obtained if the plasma density and the neutral pressure at the edge can be kept low as a result of a moderate gas fuelling. In discharges with a strong gas fuelling, high plasma edge density and neutral pressure builds up and the toroidal plasma rotation at the edge just inside the LCFS is reduced. Furthermore, measurements of density fluctuation spectra at the plasma boundary indicate a qualitative change of edge turbulence with a significant increase of fluctuations below 50 kHz. Under these conditions the edge density and the recycling flux at the main limiter start to increase prior to the global degradation. Modelling of the profile evolution after strong gas fuelling with a 1-D particle transport code shows the re-appearance of the ion temperature gradient driven mode in the plasma bulk, which is first suppressed in the transition from L- to RI-mode after impurity injection, and supports the experimental finding that the strong gas fuelling is the reason for the degradation.

1. Introduction

High density around or above the empirical Greenwald density limit [1] ($n_{GW} = I_p/\pi a^2$ with I_p the plasma current in MA and a the minor plasma radius in m giving n_{GW} in $10^{20} m^{-3}$) and energy confinement with at least H-mode quality are important requirements which must be fulfilled by an operational scenario in a future fusion reactor at the same time. H-mode discharges often show severe confinement degradation approaching n_{GW} (see e.g. discussion in [2]). However, recently it became possible to limit the degradation by increased plasma shaping [3] and even reach trans- Greenwald densities by optimised divertor pumping [4]. Alternatively, the injection of impurities can lead not only to a possible solution for the energy exhaust by the presence of a radiating belt around the plasma, but in addition to improved confinement at high plasma densities. In the Radiative Improved Mode (RI-mode) [5] at the Tokamak TEXTOR-94 the energy confinement scales linearly with the line averaged central electron density \bar{n}_e like $\tau_{RI} = K\bar{n}_e(P_{tot})^{-2/3}$ ($K = 0.18$ using s, $10^{20} m^{-3}$ and

MW as units, where P_{tot} is the total heating power). Thereby, the confinement is as good as in ELM-free H-mode discharges at $\bar{n}_e = n_{\text{GW}}$. Improved core confinement in radiative discharges is also seen in other devices [6, 7, 8]. Under RI-mode conditions the beta limit (occurring with the onset of probable neoclassical tearing modes at an empirical maximum of $\beta_n \approx 2.2$ in TEXTOR-94 [9]) is reached closely above the Greenwald limit. In TEXTOR-94 strong external gas fuelling allows to increase the density much above n_{GW} (up to a factor of 2) if MARFE formation is avoided by adjusting the horizontal plasma position and subsequently reducing the recycling at the inner wall [10]. However, at the same time strong gas fuelling generally leads to a confinement rollover and reduction down to L-mode levels at the maximum densities reached. Recently it could be shown that it is possible to optimise the energy confinement at trans- Greenwald densities in discharges with a radiating boundary [11] by careful tailoring the gas injection. In this paper we discuss the interplay between gas fuelling, plasma boundary characteristics and global performance at trans- Greenwald densities and present modelling results to describe a possible physical mechanism responsible for the confinement degradation which takes place if the gas fuelling is too strong.

2. Experimental Set-up and Discharge Scenario

TEXTOR-94 is a medium size tokamak ($R= 1.75$ m, $a= 0.46$ m) where the position of the last closed flux surface (LCFS) is determined by the toroidal belt limiter ALT-II consisting of eight pumped blades covered with carbon tiles. The RI-mode is obtained by feedback controlled neon or argon seeding under boronised wall conditions or silicon release by sputtering under siliconised wall conditions in auxiliary heated discharges (ion cyclotron resonance heating (ICRH) in combination with neutral co-beam (NBico), balanced injection by co- and counter- beam or co-beam heating alone). The deuterium gas fuelling at trans-Greenwald densities can be performed via the main fast injection system located at the wall. Alternatively, it can be performed with slower systems using inlet apertures in the ALT limiter (as described in [11]) or in a testlimiter inserted into the discharge with the help of a limiter lock at the bottom of the machine. Note, that high density discharges with the good confinement properties as described below can be obtained with each of the gas injection systems. We only concentrate on data obtained with the latter system in this paper since it is possible in this case to observe the location of the fuelling spectroscopically in TEXTOR-94. The radial profiles of electron density and temperature at the edge are determined by a thermal He- beam diagnostic located at the equatorial midplane at the low field side (LFS). The toroidal rotation has been deduced from the charge exchange recombination spectra of CVI (529 nm) using the heating beam at the same poloidal location and a spectral lamp as wavelength reference. Density fluctuations are measured with a reflectometer at the top of the machine about 2-3 cm inside the LCFS at a cut-off density of $1.7 \times 10^{19} \text{ m}^{-3}$. In this paper we discuss data obtained under boronised wall conditions using neon injection. The plasma current and toroidal field were set to $I_p = 400$ kA and $B_T = 2.25$ T ($q_a = 3.4$). The discharges were heated by ICRH and NBico with a total power of 3.0 – 3.5 MW.

3. Influence of Gas Fuelling on Confinement at High Densities

As discussed before, the maximum density in the RI-mode is given by the beta limit. Densities substantially exceeding n_{GW} can only be achieved with a degradation of the energy confinement time with respect to the one described by the RI-scaling given in section 1. Consequently, we will discuss the confinement time in terms of the ratio $\tau_E / \tau_{\text{RI}}$ later on. Note, that the RI mode confinement ($\tau_E / \tau_{\text{RI}} = 1$) is better than the one for ELM-free H-modes (characterised by $f_{\text{H93}} = \tau_E / \tau_{\text{ITERH93-P}} = 1$) at densities above n_{GW} .

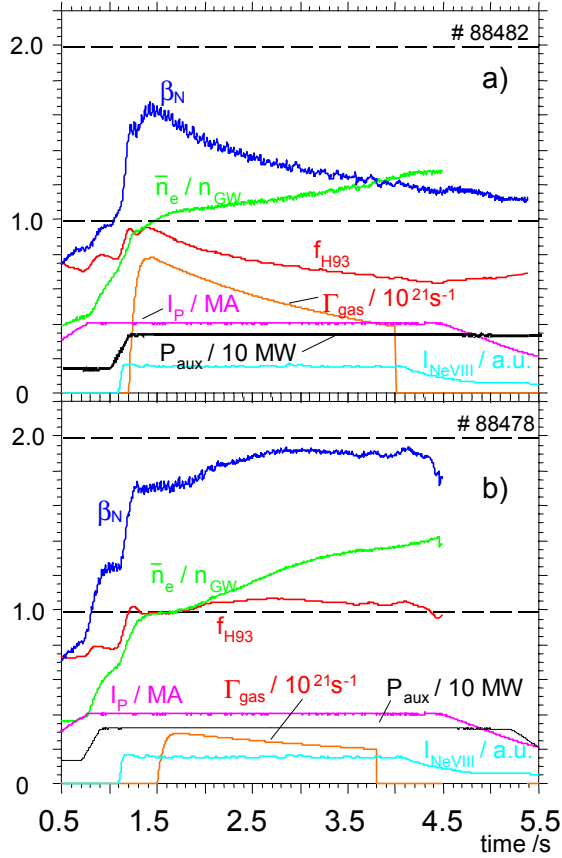


Fig 1 Time evolution of non-dimensional parameters for plasma density, pressure and energy confinement, plasma current, heating power and neon seeding for different gas fuelling rates through the testlimiter. a) max. fuelling rate $8 \times 10^{21} \text{ s}^{-1}$, b) max. fuelling rate $3 \times 10^{21} \text{ s}^{-1}$

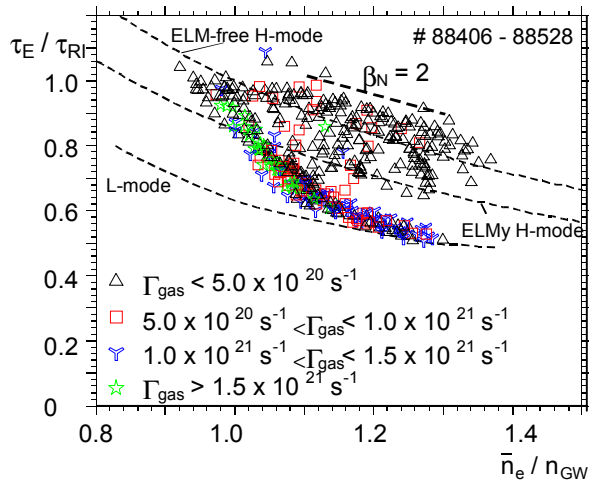


Fig. 2 Energy confinement time as a function of the Greenwald number, different symbols denote different gas fuelling rates

Figure 1 shows the sensitivity of the confinement to the D_2 fuelling rate (position of the testlimiter with the gas inlet aperture at the LCFS, $r = 0.46 \text{ m}$). The full auxiliary heating of 3.5 MW is established at 1.1 s and ends only after the current ramp down starts at 4.5 s to avoid hard disruptions at the end of these high density discharges. The neon feedback lasts from $t = 1.1$ to 4 s as indicated by the brilliance of the NeVIII line at 77 nm. The plasma density is risen by the main gas inlet up to the Greenwald limit and stops when the fuelling through the testlimiter towards trans-Greenwald densities starts. This additional gas injection takes place from 1.2 s in the discharge of fig. 1a) with a maximum fuelling rate of $8 \times 10^{21} \text{ s}^{-1}$. The plasma performance is displayed in terms of the normalised beta β_N , the Greenwald number \bar{n}_e/n_{GW} and the energy confinement time with respect to the ELM-free H-mode scaling f_{H93} (shown until the start of the current ramp down). A strong rollover of the energy confinement towards the L-mode level occurs. On the contrary, the discharge in Fig. 1b) with a smaller rate of $3 \times 10^{21} \text{ s}^{-1}$ starting at 1.5 s maintains a confinement as good as ELM-free H-modes ($f_{H93} > 1$) up to a maximum density of $\bar{n}_e/n_{GW} = 1.4$. The plasma pressure remains high at $\beta_N = 1.9$ close to the beta limit.

Figure 2 displays the ratio of the experimental energy confinement time to the RI-mode scaling as a function of the Greenwald number \bar{n}_e/n_{GW} for a large data set consisting of around 70 discharges with testlimiter fuelling and neon injection. Different symbols denote different gas injection rates, clearly illustrating that high performance at trans-Greenwald densities is only possible with moderate injection rates.

On the other hand, high gas rates lead to a confinement degradation as already shown in Fig. 1a). A confinement rollover can nevertheless also occur with low injection rates in discharges characterised by a higher wall loading with gas, caused e.g. by hard disruptions at the end of the preceding discharge.

Therefore, the best performance with moderate gas injection rates is obtained after low density recovery discharges. This ensures a subsequent low neutral edge pressure which is needed as described in the next section. The confinement times prescribed by the ELM-free, ELMy H-mode and L-mode scaling, as well as the line corresponding to $\beta_N=2$ are indicated in Fig. 2 for comparison.

4. Interplay between Plasma Edge Characteristics and Confinement

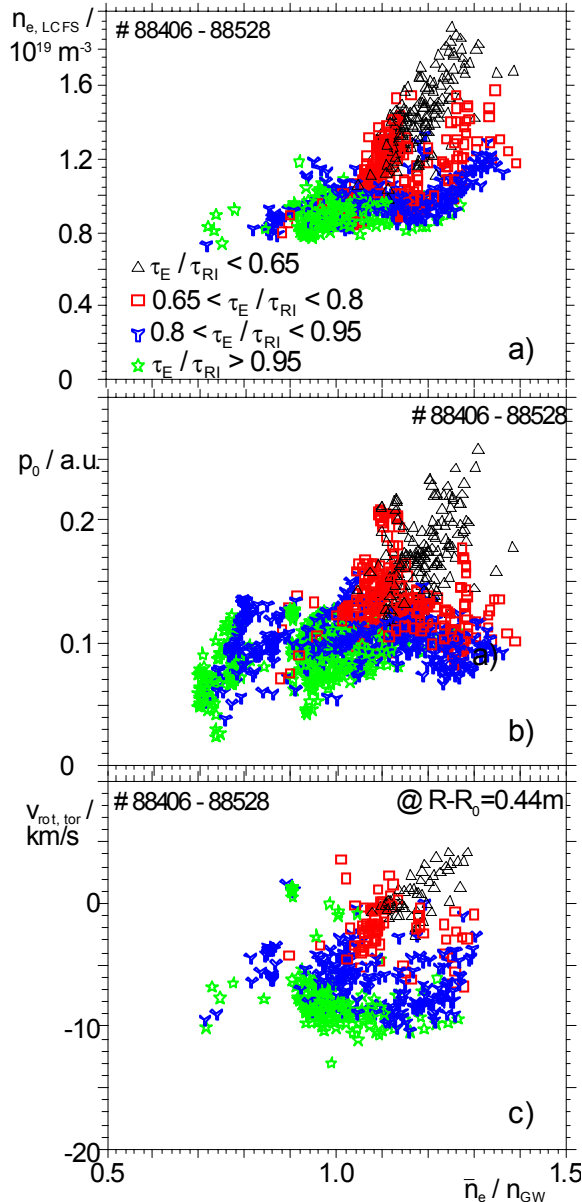


Fig 3 a) electron density at the LCFS, b) neutral pressure at the wall and c) toroidal rotation velocity as a function of the Greenwald number

The decisive influence of the plasma edge characteristics on the RI-mode performance at densities around the Greenwald limit has already been discussed earlier [12]. This influence is even more pronounced at the trans-Greenwald densities discussed here.

The edge properties show a clear correlation with the global plasma performance as seen in Fig 3 which displays as a function of the Greenwald number a) the electron density at the LCFS measured with the He- beam, b) the neutral pressure at the wall of the vessel and c) finally the velocity of toroidal plasma rotation about 2 cm inside the LCFS. All quantities are measured at the LFS in the equatorial midplane.

High performance at high densities is characterised by low edge density and neutral pressure. Under conditions of degraded confinement the density at the LCFS can be up to a factor of 1.7 higher than in discharges with comparably higher confinement (case of moderate gas fuelling). The same trend is seen in the recycling flux measured at the ALT limiter showing a strongly reduced particle confinement in the discharges with a degradation of the energy confinement.

The toroidal rotation at the edge is determined by the toroidal torque in the plasma core due to the heating beam (co- direction), the core confinement responsible for the transport of toroidal momentum to the edge, the neutrals in the edge decelerating the rotation and plasma flow in the scrape-off layer (SOL) which are in the counter direction in the outer equatorial

midplane for the normal direction of I_p and B_T ($\vec{B} \times \nabla B \downarrow$) used in these experiments. We observe, that the edge rotation is in the counter direction for discharges with high plasma performance (possibly due to the SOL flow coupling to the plasma just inside the LCFS) and almost zero under degraded conditions due to a stronger transport of toroidal momentum (in

co- direction in the core) to the edge and a reduction of the rotation due to an increased neutral density. Furthermore, we observe an interesting correlation of the density fluctuation spectra at the edge with the fuelling rate. Figure 4 shows the time evolution of the fluctuation spectra for the two discharges shown in Fig. 1. Figure 4a) corresponds to the discharge with stronger gas fuelling starting at 1.2s (cf. Fig. 1a) and followed by a confinement rollover. It displays a significant increase of low frequency fluctuations below 50 kHz which is absent in Fig. 4b) (the discharge shown in Fig 1b) where no rollover occurred). These findings give a first indication of a characteristic change of turbulence properties in the edge under conditions of strong gas fuelling in TEXTOR-94.

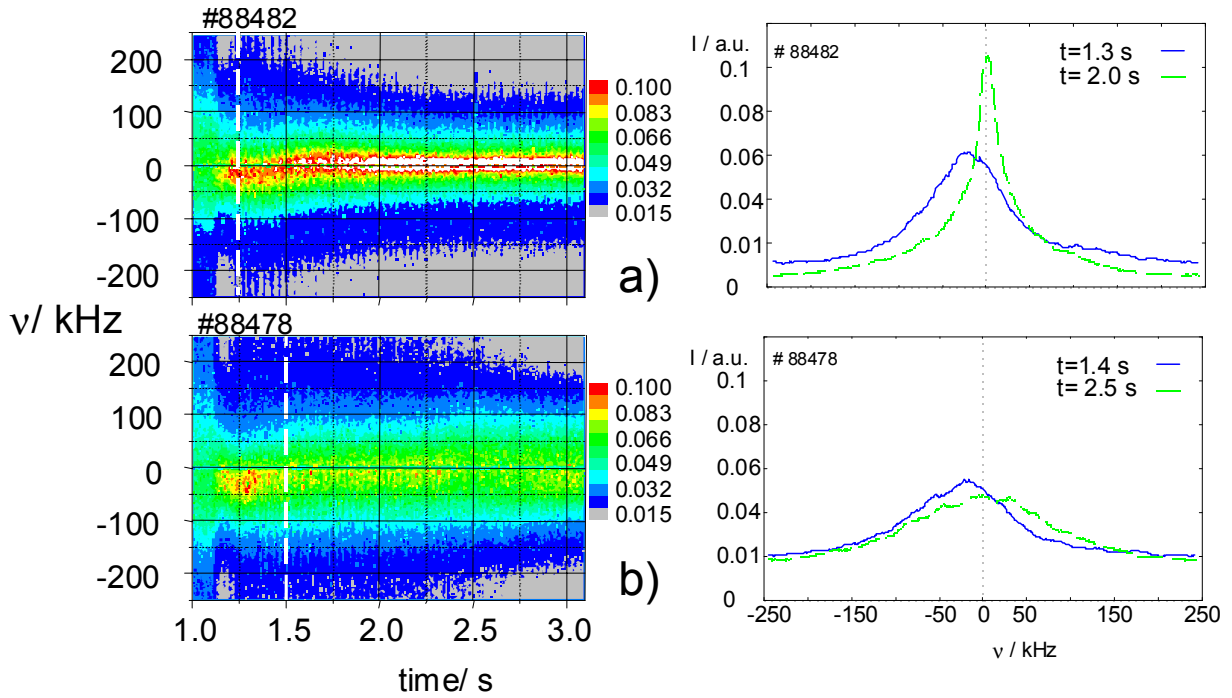


Fig 4 Time evolution of the amplitude spectra of density fluctuations measured by reflectometry (measured at the top of the machine about 2 cm inside the LCFS, cut-off density, $n_{cut} = 1.7 \times 10^{19} \text{ m}^{-3}$, frequency resolution $\Delta F = 1.95 \text{ kHz}$, time window $\Delta t = 10.24 \text{ ms}$) and the spectra at a time before (blue solid lines) and during (green dashed lines) the gas fuelling. The start of gas fuelling is indicated by vertical white lines in the time evolution, case a) discharge #88482 (strong fuelling), case b) discharge #88478 (moderate fuelling), cf. Fig 1 for discharge parameters

Naturally, an increase of edge density and neutral pressure can be expected *after* a reduction of core confinement as it is evident e.g. after confinement back transitions at the beta limit. Remarkably, the contrary is true in discharges with strong gas injection although the external gas flux is low with respect to the total flux recycling at the limiter and re-entering the plasma: The change of the plasma edge properties is *preceding* the reduction of confinement in discharges with rollover due to strong gas fuelling as shown in Fig. 5. The figure displays the time traces of the gas flow, the recycling flux at the ALT limiter, the line averaged density of an outer interferometer channel (located 6 cm inside the LCFS at the LFS), the global peaking factor of the density $n_e(0)/\langle n_e \rangle$ ($n_e(0)$ is the density on axis, $\langle n_e \rangle$ the volume averaged one) and the energy confinement time with respect to the RI-scaling τ_E/τ_{RI} (including changes of the energy content dE/dt). To exclude the modulation by the saw teeth the frequencies between 15 and 60 Hz have been filtered out for the traces in this plot.

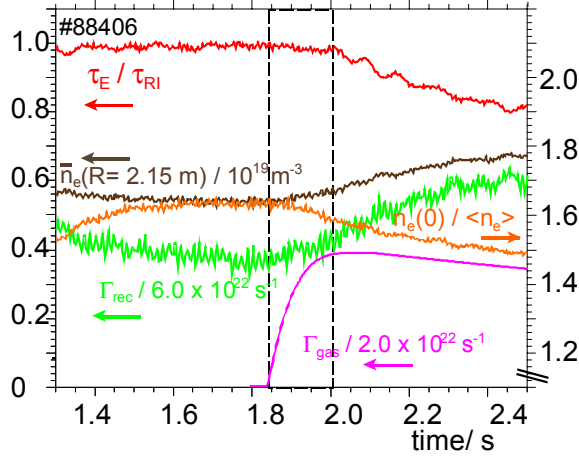


Fig 5 Time evolution of selected edge parameters and the energy confinement time with respect to the RI-scaling showing the delay of the roll over with respect to the start of the gas fuelling and the initial change of plasma edge properties

We conclude that the confinement degradation due to strong gas fuelling is initiated by processes at the plasma edge and try to illustrate the interplay between edge and global performance with the help of a model described in the next section.

5. Modelling of Confinement Degradation

The theoretical picture of the confinement improvement in the RI-mode is based on the suppression of the ion temperature gradient (ITG) mode due to the presence of the impurities and the characteristic peaking of the density profiles (caused by the particle inward pinch associated with the dissipative trapped electron mode (DTE)) [13]. The dynamic of the transition is triggered by an initial reduction of the ITG driven transport due to the increase of the effective plasma charge Z_{eff} after the impurity injection which leads to a relative increase of the transport due to DTE and an increase of the ratio between particle pinch velocity (only from DTE) and the diffusivity (from both DTE and ITG). The resulting peaking of the density profile leads to a further reduction of the ITG driven transport. The evolution of the density profile prescribed by such a 1- D model including a self- consistent description of the impurity transport and radiation during the L-RI transition in TEXTOR-94 is in good agreement with the experimental data (cf. [13] for details). Consequently, we use the same model to investigate the influence of the changes in the plasma edge occurring with strong gas fuelling on the ITG mode and the subsequent evolution of the density profile. We restrict ourselves to the description of particle transport, the temperature profiles are taken from experiment.

We start from a steady state situation in a typical RI-mode characterised by a peaked density profile and a suppression of the ITG mode over a wide radial range. The dashed lines in Fig. 6 show a) the electron density profile, b) the Z_{eff} profile and c) the diffusion coefficient due to ITG driven transport (estimated from a mixing length approximation $D = \gamma_{\text{ITG}} / k_{\text{pol}}^2 \times q^2$, where γ_{ITG} is the growth rate of the ITG mode, k_{pol} the poloidal wave number assuming $k_{\text{pol}} = 1/(2\rho_s)$, ρ_s the deuterium larmor radius and q the local safety factor). The profiles display a typical RI-mode scenario with rather peaked density profiles and a suppression of the ITG driven transport in the outer 2/3 of the minor radius. In such a scenario a strong gas flow is initiated, sufficient to increase the plasma density up to about $1.4 \times n_{\text{GW}}$, and the evolution of the density profiles is modelled. In contrast to the calculations presented in [13] where the inner 2/3 of the minor radius have been examined only, we have to include an additional description of the edge transport as turbulent transport at the edge is thought to be governed by other instabilities than ITG and DTE (e.g. ideal and resistive ballooning and interchange modes and drift waves, cf. [14] for a recent comparison of different turbulence models with experimental data). In this modelling the edge transport within a region 4 cm inside the LCFS is prescribed at by the model based on ballooning and interchange instabilities as given in [15].

However, as the plasma edge region including a transition region several cm inside the LCFS is governed by a 2D geometry and corresponding effects like particle drifts and asymmetric source distributions which are outside the scope of the model used here, a proper determination of the transport coefficients at the very edge in our 1D model is difficult and we include an ad hoc factor to scale the resulting diffusion coefficient.

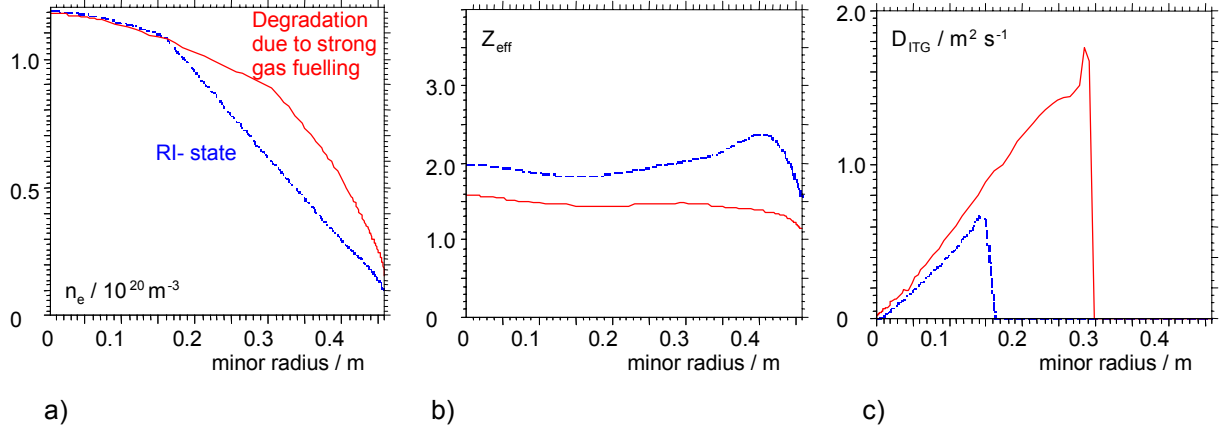


Fig. 6 Radial profiles of a) the electron density, b) the effective plasma charge and c) the diffusion coefficient resulting from the ITG mode calculated from a mixing length approximation for a RI-mode state (dashed blue lines) and for a plasma state degraded by strong gas fuelling

We modelled the evolution of the particle transport in the plasma under the assumption of an increase of the diffusion coefficient at the edge by a factor of 3 from the time of the strong gas injection on. This choice is qualitatively motivated by the experimental findings concerning the increased life time of density fluctuations at the edge and could theoretically be motivated by a possible influence of neutral particles on the growth rate of resistive ballooning modes as discussed in [16]. The increase of the edge diffusivity (influencing both the deuterium and the impurity transport) leads to a more effective screening of the impurities in the edge and a subsequent reduction of Z_{eff} over the whole profile for a given influx of neon which has been adapted to give a stationary radiation fraction of $P_{\text{rad}}/P_{\text{tot}} = 70\%$ before the additional gas fuelling starts. A reduction of Z_{eff} in discharges with a strong gas fuelling with respect to high performance discharges with moderate gas fuelling has also been observed experimentally. The time evolution modelled with the code ends in a state where the ITG mode re-appears between $r/a = 0.3$ and $r/a = 0.6$. The density profile is significantly flatter than prior the gas injection (solid lines in Fig 6 a)-c)) in agreement with the experiment (cf. evolution of the density peaking factor in Fig. 5).

If we keep the edge diffusivity unchanged after the gas fuelling for comparison, the decrease of Z_{eff} is less pronounced but the flattening of the density profile due to the additional particle source is much stronger. This situation is also characterised by the presence of ITG modes but quantitatively less in agreement with typical experimental data with respect to the shape of the density profile.

6. Summary and Conclusion

High confinement as good as in the ELM-free H-mode and high density discharges with a radiating boundary have been obtained in TEXTOR-94 by optimised gas fuelling. Moderate fuelling rates allow to keep edge density and neutral pressure sufficiently low even at densities as high as $1.4 \times n_{\text{GW}}$ without reaching the beta limit. In contrast, a confinement

rollover with high fuelling rates is observed due to a built-up of edge density and neutral pressure. Proper wall conditioning to unload the walls, however, is in addition needed to achieve the best performance and to avoid the formation of MARFEs. An increase of the density fluctuations below 50 kHz gives first indications for a qualitative change of the turbulence in the edge when strong gas fuelling is applied. Modelling indicates that the re-appearance of ITG modes in the plasma bulk is responsible for the global confinement reduction. The modelling described in this paper shows, that a possible reduction of Z_{eff} , which results in the calculation from the increased edge transport and edge density with a subsequent screening of the impurities in the edge, plays an important role for the degradation occurring with strong gas fuelling.

The experiments on high density and high confinement described in this paper confirm the decisive role of the plasma edge properties already discussed e.g. in context with the transition from saturated to improved ohmic confinement [17,18] and the performance of L-mode and supershots in TFTR [19]. Based on the experience gathered in the experiments described in this paper a new feedback circuit is presently designed at TEXTOR-94 where the gas injection to access trans-Greenwald densities will be controlled by the energy stored in the plasma. The model used to investigate the confinement rollover will be extended to describe both the particle and the energy transport which will strongly enhance its predictive capabilities.

-
- [1] M. Greenwald et al., Nucl. Fusion **28**, 2199 (1988).
 - [2] L.D. Horton et al., Nucl. Fusion **39** (1999) 1.
 - [3] L.D. Horton et al., Plasma Phys. Control. Fusion **41** (1999), B329.
 - [4] M.A. Mahdavi et al., Bull. Am. Phys. Soc. **44**, (1999) 169.
M.A. Mahdavi et al., "High Performance H-mode Plasmas at Densities above the Greenwald Limit", IAEA-CN-77/EXP1/04, these proceedings
 - [5] A.M. Messiaen et al., Phys. Rev. Lettr. **77** (1996) 2487.
 - [6] J. Ongena et al., Plasma Phys. Control. Fusion, **41** (1999) A 379.
 - [7] G.P. Maddison, „Radiating Edge Plasma Experiments on JET“, IAEA-CN-77/EX5/4, these proceedings
 - [8] G.R. McKee et al., Phys. Plasmas, **7** (2000), 1870.
M. Murakami et al., „Physics of Confinement Improvement of Plasmas with Impurity Injection in DIII-D“, IAEA-CN-77/EX5/1, these proceedings
 - [9] H.R. Koslowski et al., Nucl. Fusion **40** (2000) 821.
 - [10] J. Rapp et. al, Nucl. Fusion **39** (1999) 765.
 - [11] G. Mank et al., Phys. Rev. Lettr. **85** (2000) 2312.
 - [12] B. Unterberg et al., J. Nucl. Mater. **266-269** (1999) 75.
 - [13] M.Z. Tokar, J. Ongena, B. Unterberg and R.R. Weynants, Phys. Rev. Lettr. **85** (2000) 895.
 - [14] J.W. Connor et al., Nucl. Fusion **39** (1999) 169.
 - [15] M. Endler et al., Nucl. Fusion **35** (1995) 1307.
 - [16] A. Odblom, P.J. Catto and S.I. Krasheninnikov, Phys. Plasmas **6** (1999) 3239.
 - [17] K. Mc Cormick et al., J. Nucl. Mater. **176-177** (1990) 89.
 - [18] S. Sengoku et al., J. Nucl. Mater **176-177** (1990) 65.
 - [19] J. Strachan et al., Nucl. Fusion **39** (1999) 919.